

# Simple Ways to Obtain Activation Energy for Hydride Decomposition by Applying Data from a Volumetric Method to the Kissinger Equation

Myoung Youp SONG\*, Young Jun KWAK

Division of Advanced Materials Engineering, Hydrogen & Fuel Cell Research Center, Engineering Research Institute, Jeonbuk National University, 567 Baekje-daero Deokjin-gu Jeonju, 54896, Republic of Korea

<http://doi.org/10.5755/j02.ms.32434>

Received 6 October 2022; accepted 11 November 2022

Thermal analysis methods - such as TGA, DSC analysis, DTA, and TDS analysis - have been used in many reports to determine the activation energy for hydride decomposition. In our preceding work, we showed that the dehydriding rate of Mg-5Ni samples obeyed the first-order law and the Kissinger equation could thus be used to determine the activation energy. In the present work, we used the Mg-5Ni samples after activation. We obtained  $T_m$  at different heating rates by finding the temperature at which the ratio of the desorbed hydrogen quantity  $H_d$  change to  $T$  change,  $dH_d/dT$ , was the highest from the desorbed hydrogen quantity  $H_d$  versus temperature  $T$  curves.  $T_m$ 's at different heating rates were also obtained from points of inflection ( $\Phi = dT/dt = 0$ ) in temperature  $T$  versus time  $t$  curves. The activation energy for hydride decomposition was then calculated by applying  $T_m$ 's at different heating rates to the Kissinger equation.

**Keywords:** hydrogen storage materials, thermal analysis methods, activation energy for hydride decomposition, a volumetric method, the Kissinger equation.

## 1. INTRODUCTION

Thermal analysis methods - such as thermogravimetric analysis (TGA), differential scanning calorimetry (DSC) analysis, differential thermal analysis (DTA), and thermal desorption spectroscopy (TDS) analysis - have been used in many reports to determine the activation energy for hydride decomposition applying the Kissinger equation [1–3]. For the thermal analyses, the samples should be transferred to thermal analysis equipment after hydrogenation. To prevent the samples from being oxidized, pieces of equipment to isolate the hydrogenated samples are required. Analysis using thermal analysis equipment is not easy to be performed because evolved hydrogen is considered to contaminate parts of sensors for thermal analysis equipment. In the present work, we obtained the activation energy for the hydride decomposition of hydrided Mg-5Ni samples by applying data from a volumetric method to the Kissinger equation. This method has an advantage: data can be obtained in the same apparatus where samples were activated and hydrided.

A rate constant  $k$  is generally given by the Arrhenius equation:

$$k = Z \exp(-E/RT), \quad (1)$$

where  $Z$  is the constant,  $E$  is the activation energy,  $R$  is the gas constant, and  $T$  is the temperature.

In order that the Kissinger equation can be used to obtain the activation energy, the reaction rate equation must obey a first-order law [4, 5]. The Kissinger equation is expressed by [4, 5]:

$$\ln(\Phi/T_m^2) = \ln(ZR/E) - (E/R)(1/T_m); \quad (2)$$

$$d(\ln(\Phi/T_m^2) / d(1/T_m)) = -E/R, \quad (3)$$

where  $\Phi = dT/dt$ , the heating rate,  $T_m$  is the temperature at which the reaction rate has the maximum value, and  $E$  is the activation energy for the reaction.

Mg has many advantages as a hydrogen-storage material, but it has a low dehydriding rate even at 573 K around. To prepare a sample of Mg with increased hydriding and dehydriding rates, Ni was added, noting the reports of many researchers [6–10].

In our previous work [11], we showed that the dehydriding rate equation of Mg-5Ni samples obeyed a first-order law and the Kissinger equation could thus be used to determine the activation energy. A desorbed hydrogen quantity,  $H_d$ , was defined as the weight percentage of the desorbed hydrogen to the sample weight. In another preceding work [12], three methods from the following curves were used: (i) dehydriding rate  $dH_d/dt$  versus time  $t$  curves and  $T$  versus  $t$  curves, (ii) the ratio of  $H_d$  change to  $T$  change,  $dH_d/dT$ , versus  $T$  curves, and (iii) the ratio of  $T$  change to  $t$  change,  $dT/dt$ , versus  $t$  curves and  $T$  versus  $t$  curves.

In the present work, we used the Mg-5Ni samples after activation and simpler methods than in the work [12] to find  $T_m$ . We obtained  $T_m$  at different heating rates by finding the temperature at which the ratio of the desorbed hydrogen quantity  $H_d$  change to  $T$  change,  $dH_d/dT$ , was the highest from  $H_d$  versus temperature  $T$  curves.  $T_m$ 's at different heating rates were also obtained from points of inflection ( $\Phi = dT/dt = 0$ ) in temperature  $T$  versus time  $t$  curves. The activation energy for hydride decomposition was then calculated by applying  $T_m$ 's at different heating rates to the Kissinger equation.

\* Corresponding author. Tel.: +82-10-3260-2379; fax: +82-63-270-2386  
E-mail: [songmy@jbnu.ac.kr](mailto:songmy@jbnu.ac.kr) (M.Y. Song)

## 2. EXPERIMENTAL DETAILS

Mg [-20 + 100 mesh, 99.8 % (metals basis), Alfa Aesar] and Ni (Nickel powder APS, 2.2–3.0  $\mu\text{m}$ , purity 99.9 % metal basis, C typically < 0.1 %, Alfa Aesar) were used as starting materials. The purity of hydrogen used was 99.999 % purchased from Hankook Special Gases Co. LTD (Iksan, Republic of Korea).

For the synthesis of Mg-5Ni, milling was carried out in a planetary ball mill (Planetary Mono Mill; Pulverisette 6, Fritsch). A mixture of Mg and Ni at the weight ratio of 95:5 (total weight = 8 g) was mixed in a hermetically sealed stainless steel container (with 105 hardened steel balls, total weight = 360 g). The sample to ball weight ratio was 1:45. All sample handling was performed in a glove box under an Ar atmosphere to minimize oxidation. The mill container (volume of 250 ml) was then filled with high purity hydrogen gas (about 12 bar), which was refilled every 2 h. Milling was performed at the disc revolution speed of 400 rpm for 6 h.

Hydrogen absorption and release of Mg-5Ni were investigated using a Sievert-type volumetric apparatus, which was described previously [13]. The amount of the sample used for measurements was 0.5 g. Before dehydrogenation measurements, Mg-5Ni samples were hydrogenated at 593 K under 12 bar  $\text{H}_2$  for 60 min. The samples were cooled to room temperature in the furnace. The quantity of the hydrogen released under 1.0 bar  $\text{H}_2$  and the temperature of the reactor were measured as a function of time as the sample was heated at the heating rates ( $\Phi$ ) of 3, 6, 9, 12, and 15 K/min. The upper limit of temperature was set as 673 K.

Samples dehydrated after hydrogen absorption-release cycling were characterized by X-ray diffraction (XRD) with Cu  $\text{K}\alpha$  radiation, using a Rigaku D/MAX 2500 powder diffractometer. The microstructures of powders after reactive mechanical milling and powders dehydrated after hydrogen absorption-release cycling was observed using a JSM-5900 scanning electron microscope (SEM) operated at 20 kV.

## 3. RESULTS

Fig. 1 shows micrographs obtained by SEM at various magnifications of the Mg-5Ni sample after reactive mechanical milling. Shapes of particles are irregular. Particle size is not homogeneous. Large particles have quite flat surfaces. Particles are agglomerated. Quite small particles are on the surfaces of the particles.

Micrographs obtained by SEM at various magnifications of Mg-5Ni dehydrated after the number of cycles,  $n$ , of eight are shown in Fig. 2. Particles are in irregular shapes, having many different sizes. Particles are agglomerated. Quite small particles are found on the surfaces of the particles. The microstructure is similar to that of the sample after reactive mechanical milling (before hydrogen absorption-release cycling) except that particles have many cracks, which were formed due to expansion (by hydrogen absorption) and contraction (by hydrogen release) with cycling.

Fig. 3 shows the XRD pattern of Mg-5Ni after reactive mechanical grinding. The sample contains Mg,  $\beta\text{-MgH}_2$ ,

and Ni, and small amounts of  $\gamma\text{-MgH}_2$  and MgO. The XRD pattern of Mg-5Ni dehydrated after  $n = 8$  contained Mg and small amounts of  $\beta\text{-MgH}_2$ ,  $\text{Mg}_2\text{Ni}$ , and MgO [11].

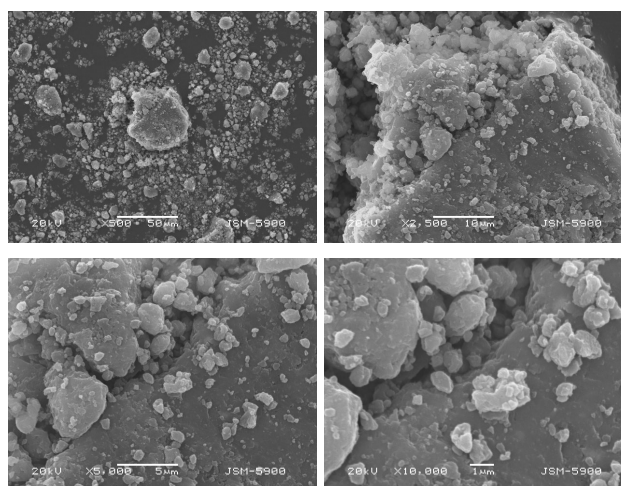


Fig. 1. Micrographs obtained by SEM at various magnifications of Mg-5Ni after reactive mechanical milling

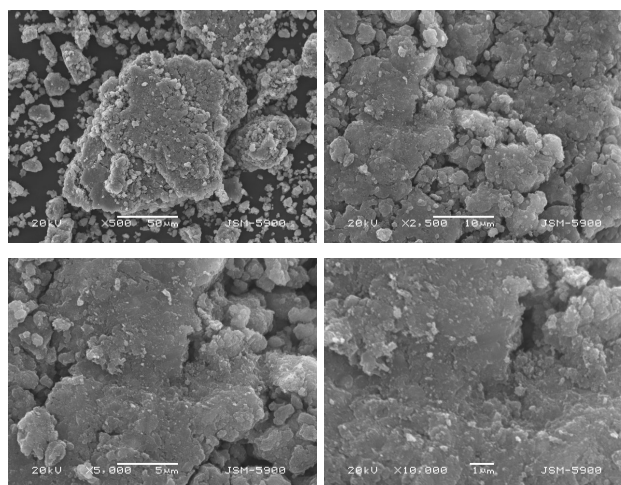


Fig. 2. Micrographs obtained by SEM at various magnifications of Mg-5Ni dehydrated after  $n = 8$

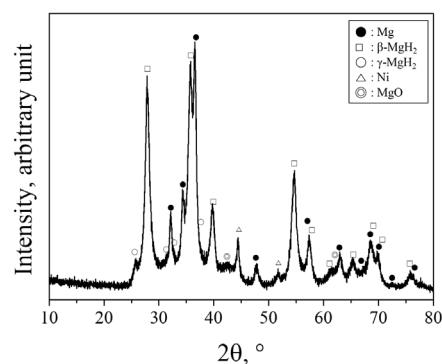


Fig. 3. XRD pattern of Mg-5Ni after reactive mechanical grinding

After hydrogen absorption-release cycles, the sample was under vacuum pumping for 1 h. The existence of the  $\beta\text{-MgH}_2$  phase shows that some Mg hydride is not decomposed even after vacuum pumping for 1 h.  $\text{Mg}_2\text{Ni}$  is believed to have been formed while the sample was heated at the first cycle [14]. The formed  $\text{Mg}_2\text{Ni}$  together with Mg

absorbs hydrogen and then releases hydrogen during hydrogen absorption-release cycling at the temperatures of this work.

The activation of the Mg-5Ni sample was completed after the third cycle ( $n = 3$ ) [10].

As the temperature of the reactor in the Sievert-type apparatus increases monotonically,  $dH_d/dT$  has a maximum value when the dehydrating rate is the highest. The temperature at which  $dH_d/dT$  has a maximum value is thus  $T_m$ .

The variation in a desorbed hydrogen quantity  $H_d$  versus temperature  $T$  curve with heating rate for hydrided Mg-5Ni after activation is shown in Fig. 4. The number of cycles,  $n$ , is indicated. Desorption begins at about 577, 584, 590, 592, and 597 K at the heating rates of 3, 6, 9, 12, and 15 K/min, respectively. Hydrogen is then released more rapidly and most rapidly at the temperature where about 18.7 % of the total absorbed quantity of hydrogen is released. Thereafter the sample releases hydrogen less rapidly and finally the dehydrating rate becomes very low. As the number of cycles increases, the total absorbed quantity of hydrogen decreases. It is believed that the decrease in the total absorbed quantity of hydrogen is because a part of Mg is oxidized to form MgO and the particles agglomerate when the temperature reaches relatively high temperatures.

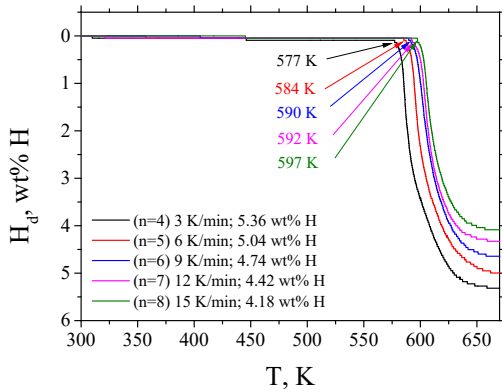


**Fig. 4.** Variation in a desorbed hydrogen quantity  $H_d$  versus temperature  $T$  curve with a heating rate for hydrided Mg-5Ni after activation

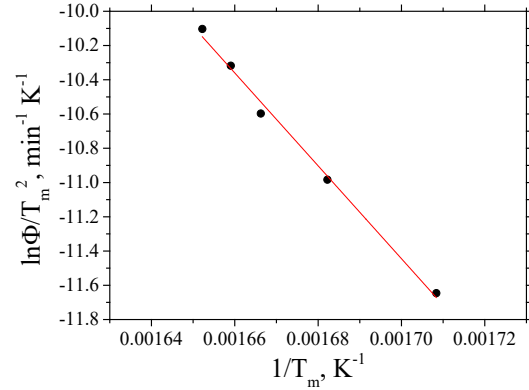
The ratio of the desorbed hydrogen quantity  $H_d$  change to  $T$  change,  $dH_d/dT$ , was the highest when about 18.7 % of the total absorbed quantity of hydrogen was released.  $T_m$  was thus the temperature when 18.7 % of the total absorbed quantity of hydrogen was released. At heating rates of 3, 6, 9, 12, and 15,  $T_m$ 's were the temperatures when  $H_d = 1.02, 0.93, 0.88, 0.84,$  and  $0.79$  wt.% H, respectively.

Table 1 shows the variations in  $T_m$ ,  $\ln(\Phi/T_m^2)$ , and  $1/T_m$ , with heating rate  $\Phi$  under 1.0 bar  $H_2$  for hydrided Mg-5Ni after activation, obtained from the temperature when 18.7 % of the total absorbed quantity of hydrogen was released.

Fig. 5 shows the plot of  $\ln(\Phi/T_m^2)$  versus  $1/T_m$ , obtained from the data of  $H_d$  versus  $T$  curves. The linearity of the plot is very good (correlation coefficient: 0.997). The activation energy for hydride decomposition,  $E$ , was calculated as 225 kJ/mol from this plot.

**Table 1.** Variations in  $T_m$ ,  $\ln(\Phi/T_m^2)$ , and  $1/T_m$ , with heating rate  $\Phi$  under 1.0 bar  $H_2$  for hydrided Mg-5Ni after activation, obtained from the temperature when 18.7 % of the total absorbed quantity of hydrogen was released

$\Phi$ , K min <sup>-1</sup>	$H_d$ , wt.% H	$T_m$ , K	$\ln(\Phi/T_m^2)$ , K <sup>-2</sup> min <sup>-1</sup>	$1/T_m$ , K <sup>-1</sup>
3	1.02	585.35	-11.646	0.0017084
6	0.93	594.45	-10.984	0.0016822
9	0.88	600.15	-10.597	0.0016663
12	0.84	602.75	-10.318	0.0016591
15	0.79	605.25	-10.103	0.0016522



**Fig. 5.** Plot of  $\ln(\Phi/T_m^2)$  versus  $1/T_m$ , obtained from the data of  $H_d$  versus  $T$  curves

Now we try another way to calculate  $E$  from data obtained in a Sievert-type apparatus.  $T_m$  will be obtained from  $T$  versus  $t$  curves. The difference in heat between the heat supplied by the furnace and the heat absorbed by the sample for hydride decomposition will increase the temperature of the reactor. When hydrides do not decompose, all the heat supplied by the furnace will increase the temperature of the reactor. When the reaction begins, a part of the heat will be used for hydride decomposition, leading to a slower increase in the temperature of the reactor. At the moment when all the heat supplied by the furnace is consumed for hydride decomposition, the temperature of the reactor will not increase and stay constant. This is the temperature when  $dT/dt$  is zero (a point of inflection in  $T$  versus  $t$  curve) and when the sample has the maximum hydride decomposition rate. Thus, the temperature at which  $dT/dt$  is zero in  $T$  versus  $t$  curves is  $T_m$ . After  $T_m$ , the temperature of the reactor will increase because less and less heat will be used for hydride decomposition.

$T$  versus  $t$  curves for hydrided Mg-5Ni after activation when heated with a heating rate of 3, 6, 9, 12, and 15 K/min are shown in Fig. 6. From these curves,  $T_m$ 's were obtained. The temperature increases slowly and then quite rapidly, reaching the heating rate programmed. At some point the temperature increases less rapidly and arrives at a temperature where the temperature remains constant. This is the point for  $T_m$ , which is a point of inflection in the  $T$  versus  $t$  curve. After passing the point of inflection, the temperature increases slowly and reaches again the heating rate programmed. And finally, the temperature increases less rapidly and then stays unchanged because the temperature limit was set as 673 K.

Table 2 shows the variations in  $T_m$ ,  $\ln(\Phi/T_m^2)$ , and

$1/T_m$ , with heating rate  $\Phi$  under 1.0 bar  $H_2$  for hydrided Mg-5Ni after activation, obtained from the data of  $T$  versus  $t$  curves.

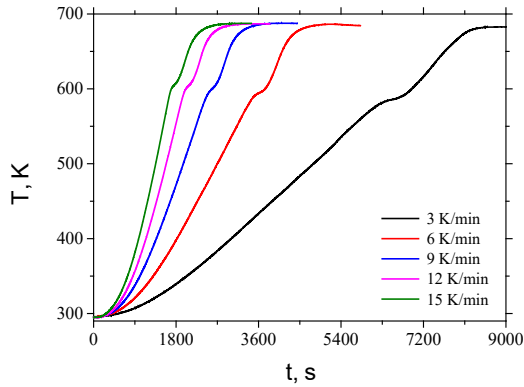


**Fig. 6.**  $T$  versus  $t$  curves for hydrided Mg-5Ni after activation when heated with a heating rate of 3, 6, 9, 12, and 15 K/min

**Table 2.** Variations in  $T_m$ ,  $\ln(\Phi/T_m^2)$ , and  $1/T_m$ , with heating rate  $\Phi$  under 1.0 bar  $H_2$  for hydrided Mg-5Ni, obtained from the data of  $T$  versus  $t$  curves.

$\Phi$ , K min <sup>-1</sup>	$T_m$ , K	$\ln(\Phi/T_m^2)$ , K <sup>-1</sup> min <sup>-1</sup>	$1/T_m$ , K <sup>-1</sup>
3	585.00	-11.645	0.0017094
6	595.00	-10.985	0.0016807
9	600.00	-10.597	0.0016667
12	603.50	-10.321	0.0016570
15	606.00	-10.106	0.0016502

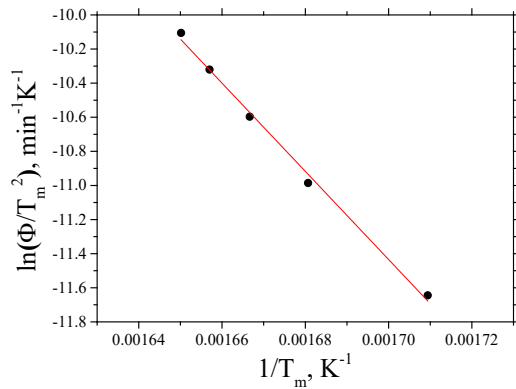


**Fig. 7.** Plot of  $\ln(\Phi/T_m^2)$  versus  $1/T_m$ , obtained from the data of  $T$  versus  $t$  curves

Fig. 7 shows the plot of  $\ln(\Phi/T_m^2)$  versus  $1/T_m$ , obtained from the data of  $T$  versus  $t$  curves. The linearity of the plot is very good (correlation coefficient: 0.998). From this plot, the activation energy for hydride decomposition,  $E$ , was calculated as 215 kJ/mol. The margin of error was relatively large.

#### 4. DISCUSSION

As Mg-based hydrogen storage materials [15, 16], many works were performed in our laboratory to increase the hydrogenation and dehydrogenation rates of Mg by adding metallic elements or compounds [17–20], which form defects and clean surfaces and decrease the particle size. In this work, 5 wt.% Ni-added Mg samples, Mg-5Ni samples, were prepared.

The sample dehydrided after  $n = 8$  contained Mg and small amounts of  $\beta$ -MgH<sub>2</sub>, Mg<sub>2</sub>Ni, and MgO. Neglecting the quantity of MgO, the composition of the sample was 97.8 mol% Mg + 2.2 mol % Mg<sub>2</sub>Ni. Mg and Mg<sub>2</sub>Ni absorb hydrogen and then release hydrogen during hydriding-dehydriding cycling under the conditions of the present work.

Particles after  $n = 8$  have many cracks, which were formed due to expansion and contraction with hydrogen absorption-release cycling.

In the  $T$  versus  $t$  curves of Fig. 6, a point of inflection appears. The temperature at this point is  $T_m$ . At the end of the  $T$  versus  $t$  curves, the temperature increases less rapidly because, even though the hydride decomposition reaction stops, less heat is supplied by the furnace since the temperature limit is set as 673 K in the program of the temperature controller.

Now we'll mention the result of our previous work [11], in which the obtained activation energy for hydride decomposition was 174 kJ/mol, which is smaller than those obtained in this work. In that work [11],  $T_m$  was obtained assuming that  $T_m$  was the temperature at the time corresponding to the center of the asymmetric peak. This assumption is thought to have led to a different result, which was shown to be incorrect by the results of the present work.

$T_m$ 's were obtained at different heating rates by finding the temperature at which  $dH_d/dT$  is the highest from the  $H_d$  versus  $T$  curves.  $T_m$ 's at different heating rates were also obtained from points of inflection in the  $T$  versus  $t$  curves. These methods to obtain  $T_m$  are simpler than the method used in our previous work [12].

The Mg-5Ni sample is composed of approximately 97.8 mol% Mg and 2.2 mol% Mg<sub>2</sub>Ni. Because it was hard to find the results of the samples with compositions similar to Mg-5Ni and the mol% of Mg<sub>2</sub>Ni is relatively small, we compared the results of this work with those of MgH<sub>2</sub>. The activation energies for dehydrogenation (225 and 215 kJ/mol) of the hydrogenated Mg-5Ni samples obtained in the present work are larger than that of Zhao-Karger et al. [1] for the hydrogen release of the commercial MgH<sub>2</sub> (195 kJ/mol) and that of Sabitu and Goudy [2] for MgH<sub>2</sub> decomposition of MgH<sub>2</sub> without oxide (174 kJ/mol), but smaller than that of Campostrini et al. [21] for the hydrogen release of the commercial MgH<sub>2</sub> powders (240 kJ/mol). Our result has a value similar to that of Xiao et al. [22] for MgH<sub>2</sub> decomposition of an as-received MgH<sub>2</sub> (213 kJ/mol).

For the thermal analyses, transferring of the samples after isolation is required and danger of contamination for the sensors exists. The volumetric method is simpler because data can be obtained in the same apparatus where samples were hydrided. In this work, we obtained  $T_m$ 's from  $H_d$  versus  $T$  curves and  $T$  versus  $t$  curves which were obtained from the volumetric method.

#### 5. CONCLUSIONS

We proposed simple ways to obtain the activation energy for hydride decomposition of the hydrided Mg-5Ni sample after activation by applying data from a volumetric method to the Kissinger equation. In our previous work,

we showed that the dehydrodring rate equation of Mg-5Ni samples obeyed the first-order law and the Kissinger equation could thus be used to determine the activation energy. The composition of the sample was approximately 97.8 mol% Mg + 2.2 mol% Mg<sub>2</sub>Ni. We obtained  $T_m$  at different heating rates by finding the temperature at which the ratio of the desorbed hydrogen quantity  $H_d$  change to  $T$  change,  $dH_d/dT$ , is the highest from the desorbed hydrogen quantity  $H_d$  versus temperature  $T$  curves. The activation energy was calculated as 225 kJ/mol.  $T_m$ 's at different heating rates were also obtained from points of inflection in temperature  $T$  versus time  $t$  curves. The activation energy was calculated as 215 kJ/mol.

## REFERENCES

1. Zhao-Karger, Z., Hu, J., Roth, A., Wang, D., Kubel, C., Lohstroh, W., Fichtner, M. Altered Thermodynamic and Kinetic Properties of MgH<sub>2</sub> Infiltrated in Microporous Scaffold *Chemical Communications* 46 2010: pp. 8353–8355. <https://doi.org/10.1039/C0CC03072D>
2. Sabitu, S.T., Goudy, A.J. Dehydrogenation Kinetics and Modeling Studies of MgH<sub>2</sub> Enhanced by Transition Metal Oxide Catalysts Using Constant Pressure Thermodynamic Driving Forces *Metals* 2 2012: pp. 219–228. <https://doi.org/10.3390/met2030219>
3. Figen, A.K., Coskuner, B., Piskin, S. Hydrogen Desorption Kinetics of MgH<sub>2</sub> Synthesized from Modified Waste Magnesium *Materials Science* 32 2014: pp. 385–390. <https://doi.org/10.2478/s13536-014-0218-9>
4. Kissinger, H.E. Variation of Peak Temperature with Heating Rate in Differential Thermal Analysis *Journal of Research of the National Bureau of Standards* 4 1956: pp. 217–221. <https://doi.org/10.6028/jres.057.026>
5. Blainea, R.L., Kissinger, H.E. Homer Kissinger and the Kissinger equation *Thermochimica Acta* 540 2012: pp. 1–6. <https://doi.org/10.1016/j.tca.2012.04.008>
6. Bobet, J.L., Akiba, E., Darriet, B. Study of Mg-M (M=Co, Ni and Fe) Mixture Elaborated by Reactive Mechanical Alloying: Hydrogen Sorption Properties *International Journal of Hydrogen Energy* 26 2001: pp. 493–501. [https://doi.org/10.1016/S0360-3199\(00\)00082-3](https://doi.org/10.1016/S0360-3199(00)00082-3)
7. Santos, S.F., Ishikawa, T.T., Botta, W.J., Huot, J. MgH<sub>2</sub> + FeNb Nanocomposites for Hydrogen Storage *Materials Chemistry and Physics* 147 2014: pp. 557–562. <https://doi.org/10.1016/j.matchemphys.2014.05.031>
8. Asselli, A.A.C., Santos, S.F., Huot, J. Hydrogen Storage in Filled Magnesium *Journal of Alloys and Compounds* 687 2016: pp. 586–594. <https://doi.org/10.1016/j.jallcom.2016.06.109>
9. Bobet, J.L., Akiba, E., Nakamura, Y., Darriet, B. Study of Mg-M (M=Co, Ni and Fe) Mixture Elaborated by Reactive Mechanical Alloying-Hydrogen Sorption Properties *International Journal of Hydrogen Energy* 25 2000: pp. 987–996. [https://doi.org/10.1016/S0360-3199\(00\)00002-1](https://doi.org/10.1016/S0360-3199(00)00002-1)
10. Yu, Z., Zhang, W., Zhang, Y., Fu, Y., Cheng, Y., Guo, S., Li, Y., Han, S. Remarkable Kinetics of Novel Ni@CeO<sub>2</sub>-MgH<sub>2</sub> Hydrogen Storage Composite *International Journal of Hydrogen Energy* 47 2022: pp. 35352–35364. <https://doi.org/10.1016/j.ijhydene.2022.08.121>
11. Song, M.Y., Kwak, Y.J. Determination of the Activation Energy for Hydride Decomposition Using a Sieverts-Type Apparatus and the Kissinger Equation *Metals* 12 2022: pp. 265. <https://doi.org/10.3390/met12020265>
12. Song, M.Y., Kwak, Y.J. Three Methods for Application of Data from a Volumetric Method to the Kissinger Equation to Obtain Activation Energy *Micromachines* 13 2022: pp. 1809. <https://doi.org/10.3390/mi13111809>
13. Song, M.Y., Kwak, Y.J., Lee, S.H., Park, H.R. Enhancement of Hydrogen Storage Characteristics of Mg by Addition of Nickel and Niobium (V) Fluoride via Mechanical Alloying *Korean Journal of Metals and Materials* 54 2016: pp. 210–216. <https://doi.org/10.3365/KJMM.2016.54.3.210>
14. Song, M.Y., Ivanov, E.I., Darriet, B., Pezat, M., Hagenmuller, P. Hydriding Properties of a Mechanically Alloyed Mixture with a Composition Mg<sub>2</sub>Ni *International Journal of Hydrogen Energy* 10 1985: pp. 169–178. [https://doi.org/10.1016/0360-3199\(85\)90024-2](https://doi.org/10.1016/0360-3199(85)90024-2)
15. Kim, M.G., Han, J.H., Lee, Y.H., Son, J.T., Hong, T.W. Hydrogenation Properties of MgH<sub>2</sub>-CaO Composites Synthesized by Hydrogen-Induced Mechanical Alloying *Korean Journal of Metals and Materials* 56 2018: pp. 829–834. <https://doi.org/10.3365/KJMM.2018.56.11.829>
16. Han, J.S., Park, K.D. Thermal Analysis of Mg Hydride by Sievert's Type Automatic Apparatus *Korean Journal of Metals and Materials* 48 2010: pp. 1123–1129. <https://doi.org/10.3365/KJMM.2010.48.12.1123>
17. Song, M.Y., Lee, S.H., Kwak, Y.J. Improvement in the Hydrogenation and Dehydrogenation Features of Mg by Milling in Hydrogen with Vanadium Chloride *Korean Journal of Metals and Materials* 10 2021: pp. 709–717. <https://doi.org/10.3365/KJMM.2021.59.10.709>
18. Song, M.Y., Choi, E.H., Kwak, Y.J. Increase in the Dehydrogenation Rates and Hydrogen-Storage Capacity of Mg-Graphene Composites by Adding Nickel via Reactive Ball Milling *Materials Research Bulletin* 130 2020: pp. 110938. <https://doi.org/10.1016/j.materresbull.2020.110938>
19. Song, M.Y., Kwak, Y.J. Hydrogen Charging Kinetics of Mg – 10 wt% Fe<sub>2</sub>O<sub>3</sub> Prepared via MgH<sub>2</sub>-Forming Mechanical Milling *Materials Research Bulletin* 140 2021: pp. 111304. <https://doi.org/10.1016/j.materresbull.2021.111304>
20. Song, M.Y., Kwak, Y.J., Choi, E. Rate-Controlling Steps for the Hydriding Reaction of an Intermetallic Compound Mg<sub>2</sub>Ni *Journal of Nanoscience and Nanotechnology* 20 2020: pp. 7010–7017. <https://doi.org/10.1166/jnn.2020.18840>
21. Campostrini, R., Abdellatif, M., Leoni, M., Scardi, P. Activation Energy in the Thermal Decomposition of MgH<sub>2</sub> Powders by Coupled TG-MS Measurements *Journal of Thermal Analysis and Analytical Calorimetry* 116 2014: pp. 225–240. <https://doi.org/10.1007/s10973-013-3539-8>
22. Xiao, X., Liu, Z., Yarahmadi, S.S., Gregorya, D.H. Facile Preparation of β-/γ-MgH<sub>2</sub> Nanocomposites under Mild Conditions and Pathways to Rapid Dehydrogenation *Physical Chemistry Chemical Physics* 18 2016: pp. 10492–10498. <https://doi.org/10.1039/C5CP07762A>



© Song et al. 2023 Open Access This article is distributed under the terms of the Creative Commons Attribution 4.0 International License (<http://creativecommons.org/licenses/by/4.0/>), which permits unrestricted use, distribution, and reproduction in any medium, provided you give appropriate credit to the original author(s) and the source, provide a link to the Creative Commons license, and indicate if changes were made.